Available online at www.sciencedirect.com
SCIENCE DIRECT
Dyes and Pigments 72 (2007) 185–191
DYES and PIGMENTS
www.elsevier.com/locate/dyepig

A TD-DFT investigation of the visible spectra of fluoro-anthraquinones

Julien Preat*[,1], Denis Jacquemin [2], Eric A. Perpète [2]

Laboratoire de Chimie Théorique Appliquée, Facultés Universitaires Notre-Dame de la Paix, rue de Bruxelles, 61, 5000 Namur, Belgium

Received 11 April 2005; accepted 19 August 2005
Available online 10 October 2005

Abstract

With ab initio computational chemistry techniques explicitly taking into account electron correlation and solvent effects, we investigate the chemical substitution impact on the λ_{max} of absorption, of 1,2,3,4-tetrafluoro-9,10-anthraquinone. Increasing the electron-donating strength of the auxochromic groups leads to bathochromic displacements. The largest bathochromic effect has been observed when four built-up hydrogen bonds interact with the C═O chromophores. For each substitution, the results are rationalized in terms of HOMO and LUMO energy levels, as well as in hydrogen bond effects on the charge separation and bond length in the chromophoric unit.

Keywords: Anthraquinone; Density-functional theory; Electronic spectra; Fluorinated dyes; Hydrogen bond

1. Introduction

The carbonyl class of dyes is largely used under a variety of chemical forms: coumarins, perinones, quinacridones… having in common the C═O group which may be considered as an essential chromophoric unit. These dyes owe their success to (i) their ability to provide a wide range of colours, covering the entire visible spectrum and (ii) their capacity to show long wavelength absorption bands when combined with relatively short π-conjugated system. For instance, 9,10-anthraquinone (AQ) derivatives, in which the central ring bearing two carbonyl groups is fused to two fully aromatic six-membered rings, can give rise to a complete range of shades, depending on the nature and relative position(s) of the auxochromic group(s) substituting hydrogen atom(s) on the outer rings [1]. For these reasons, it is a major precursor of many dyes used in the tinctorial industry [2]. In particular, fluorinated compounds may show unique properties, like near-infrared absorption and could therefore be potential candidates in the CD-R and DVD-R applications [3,4].

As a predictive tool of targeted properties, the modern molecular modelization techniques nowadays offer a competitive solution for the interpretation of experimental data. Actually, the accurate prediction of UV/VIS spectra of large molecules is still a domain of concern [5]. The improved CPU resources availability now allow to study, at correlated levels of approximation, the absorption spectra of large molecular species, such as the anthraquinoïdic dyes. The most widely used ab initio approach in UV/VIS calculations is the time-dependent density-functional theory (TD-DFT) which, for a reasonable computational effort, commonly yields to accurate results, especially when hybrid functionals (see below) are used [6–17].

The present work aims at rationalizing and predicting with accuracy, the λ_{max} of a series of 1,2,3,4-tetrafluoro-9,10-anthraquinone derivatives that have recently been synthesized by Matsui and coworkers [4] (Fig. 1, Table 1). In addition to the synthesis of the fluoro-dyes, they have provided a first theoretical analysis of the UV/VIS spectra following the theoretical scheme: (i) first, the geometry of all compounds is optimized with the B3LYP/3-21G method, (ii) the absorption

* Corresponding author. Tel.: +32 81 724568; fax: +32 81 724567.
E-mail addresses: julien.preat@fundp.ac.be (J. Preat), denis.jacquemin@fundp.ac.be (D. Jacquemin), eric.perpete@fundp.ac.be (E.A. Perpète).
[1] Fellow of the Belgian National Fund for the Formation to Research in Industry and Agriculture (FRIA).
[2] Research Associate of the Belgian National Fund for Scientific Research (FNRS).

0143-7208/$ - see front matter © 2005 Elsevier Ltd. All rights reserved.
doi:10.1016/j.dyepig.2005.08.015

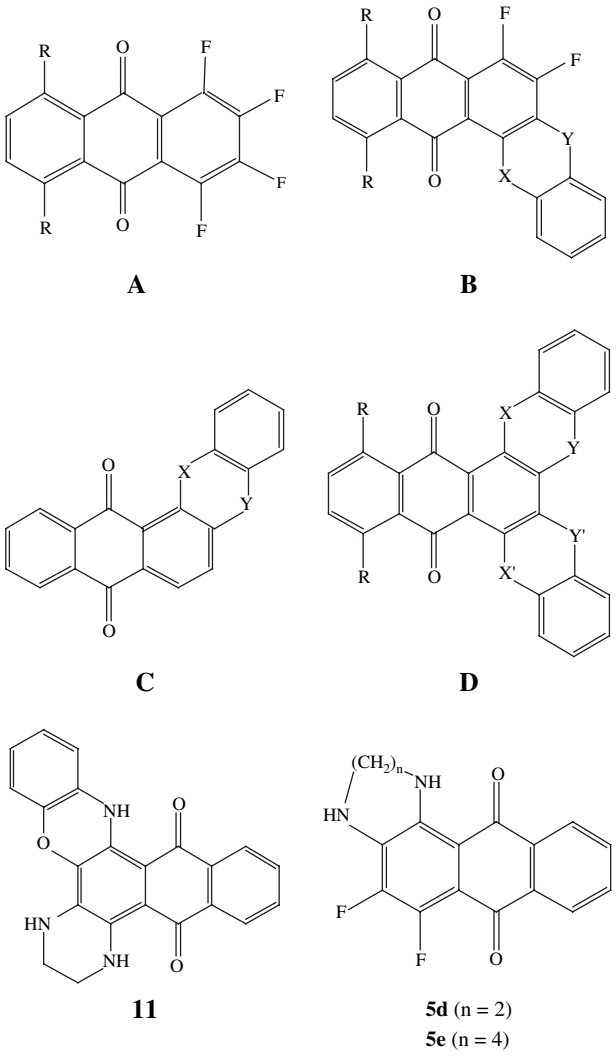

Fig. 1. Chemical structure of the studied anthraquinone in this calculation. We used same number than in Ref. [4].

spectra are produced with the semi-empirical INDO/S method. It turns out that on their selected molecular set, this strategy leads to an average discrepancy of 123 nm between theoretical and experimental λ_{max}. In this work, we show that this methodology can significantly be improved if one uses better levels of approximation, even when increasing the size of the investigated molecular set. Consequently, we focus on the chromic effect of each fluoro atom substitution and, on the other hand, we consider the other side of the molecule (i.e., the 5, 6, 7 and 8 substitution positions).

2. Methodology

All calculations have been performed with the Gaussian 03 [18] package, following the methodological procedure described in our previous study of 9,10-anthraquinone dyes [6]: (i) the optimization of the ground-state geometry, (ii) the determination of the vertical electronic excitation energies. The ground-state optimizations have been performed with DFT, while the excitation spectra are evaluated with TD-DFT. DFT

Table 1
Recapitulative of the studied anthraquinone derivatives

Compound	Type	R	X	Y	X′	Y′
1	**A**	H				
2	**A**	OH				
3	**A**	Cl				
5a	**B**	H	NH	O		
5b	**B**	H	O	O		
5c	**B**	H	NH	S		
5c′	**C**	H	NH	S		
6a	**B**	OH	NH	O		
6b	**B**	OH	O	O		
6c	**B**	OH	NH	S		
7c	**B**	Cl	NH	S		
8	**D**	H	NH	O	NH	O
9	**D**	H	NH	O	O	O
10	**D**	H	NH	O	NH	S
12	**D**	H	O	O	O	O
13	**D**	H	O	O	NH	S
14	**D**	H	NH	S	NH	S
15	**D**	Cl	NH	S	NH	S
18	**B**	H	O	NH		
19	**D**	H	S	S	S	S
20	**B**	H	O	S		
21	**D**	SH	NH	S	NH	S
22	**D**	OH	NH	S	NH	S
23	**D**	NH_2	NH	S	NH	S

orbitals are obtained by solving the Kohn–Sham equation, involving exchange and correlation (XC) terms. Numerous XC functionals have been developed and an adequate choice is crucial to obtain reliable results. In a first group, one finds the local density approximation (LDA) functionals. In this scheme, a potential due to a spherical and uniform distribution of the density of charge is given to each electron: this approximation is often inappropriate for studying the excitation spectra [6]. In a second group, one finds the gradient corrected functionals (GGA for generalized gradient approximation), for example BLYP (Becke's exchange [19] and Lee, Yang, Parr (LYP) [20] correlation) and PBE (Perdew–Burke–Erzenrhof) [21,22]. In this scheme, the exchange–correlation potential is a function of both the density and its gradient. Even if compared to LDA's, GGA functionals provide superior results, they are unable to deliver correct values for most of the dye properties (geometry, UV/VIS spectrum). In a third group one finds hybrid functionals that currently have the favours of the computational chemists, and include a fraction of *exact* (i.e., Hartree–Fock (HF)) exchange. Typically, the so-called three-parameter hybrids are built like:

$$E^{\mathrm{XC}} = E^{\mathrm{LDA\text{-}XC}} + \beta_1\left(E^{\mathrm{HF\text{-}X}} - E^{\mathrm{LDA\text{-}X}}\right) + \beta_2 \Delta E^{\mathrm{GGA\text{-}X}} + \beta_3 \Delta E^{\mathrm{GGA\text{-}C}} \quad (1)$$

where the GGA corrections on the exchange and correlation energies explicitly appear. The β_i parameters are often optimized with a method of least-squares fitting on experimental data (atomization enthalpies, ionization potentials, electroaffinities,…). In this work, we used B3LYP [20,23] ($\beta_1 = 0.20$, $\beta_2 = 0.72$, $\beta_3 = 0.83$) and PBE0 [24,25]

($\beta_1 = 0.25$, $\beta_2 = 0.50$, $\beta_3 = 1.00$). From our previous investigation, we have selected the 6-31G(d,p) [26] basis set, that has been shown able to reproduce the λ_{max} of −OH, $-NH_2$, −Cl and −Me AQ-derivatives [6].

In Ref. [6], we demonstrate that although they do not significantly affect the geometry of anthraquinone dyes, the solvation effects have to be taken into account for accurately computing their UV/VIS spectra. Consequently, the polarizable continuum model (PCM) developed in Torino and Pisa [18,27] is used for evaluating the bulk solvent effects. In PCM, one divides the problem into a solute part (anthraquinone) lying inside a cavity, and a solvent part (in our case dichloromethane) represented as a structureless material, characterized by its dielectric constant, as well as other parameters. PCM is able to obtain a valid approximation of solvent effects as long as no specific interaction between the solute and the solvent exists. In this work, we used the so-called non-equilibrium PCM solution [7].

To reach the best agreement between theory and experiment (including the effects of solute−solvent specific interactions), the results of different approaches are combined by means of a multilinear regression (MLR) scheme. MLR is based on the numerical technique of least-squares fitting and analyses the relationship between one dependent variable (experimental value) and one or more independent variables (theoretical values or properties) [28–30]. To test the significance of a regression, the total sum of squares (TSS) is split into two components, the model sum of squares (MSS) and the residual sum of squares (RSS). If the mathematical model passes through all the original data points, the MSS is equal to the TSS and the RSS is zero. The test calculations are carried out in a so-called ANalysis Of the VAriance table (ANOVA). The confidence limits for the regression parameters (b_i) measure the adequacy of each independent variable in the model. The ratio between b_i and the associated error could be compared to a critical value for which the probability (P-value) to reject the model has been tabulated. This treatment allows to eliminate step by step the less significant independent variables. In this study, MLR has been performed with the *Statgraphics Plus 5.1* program [31].

3. Results

3.1. Molecular geometry

A characteristic feature of the absorption spectra of numerous AQ-derivatives is the existence of several maxima in the long-wave band. Many suggestions have been made to elucidate this spectral pattern [32–34]. Our favour goes to the vibrational coupling hypothesis because the distance between the two neighbouring peaks very often sticks to an infrared frequency. For instance, one can check that the typical $\sim 1250\ cm^{-1}$ stretching of secondary amino side group corresponds to ~ 45 nm separation experimentally observed for 1,4-diamino-AQ [35]. Therefore, we could theoretically simulate this λ_{max} progression by performing a vibrational analysis on the excited state, but this stands far beyond the scope of this paper. Previous works on AQ-dyes [4,6,10] have shown that the excitation process is related to an enhancement of the charge separation in the naphthoquinone chromophoric unit. Schematically, one goes from a polarized C=O ground state to a zwitterionic limit C^+-O^- in the excited state. The magnitude of this charge separation, as well as its stabilization are directly related to the position and the height of the absorption band. Several factors can be assessed that would favour such an ionic structure, make it less energetic and consequently batho-shift the corresponding λ_{max}. For instance, grafting an electron-active side group allows C^+-O^- to be stabilized by delocalization of the charge around the AQ-core: many mesomeric forms can be written. Any hydrogen bond, typically set up by 1, 4, 5 or 8-substitution will bring an extra stabilization of the negative charge borne by the oxygen atom. Furthermore, surrounding solvent molecules (or the medium) can help diluting into the bulk the excess charge of the carbonyl oxygen atoms.

First, we assess the coplanarity of the anthraquinone core with the side fused cycles. To test the planarity, we start the geometry optimization from non-planar structures and, after the minimization process, we perform a vibrational analysis to check that no imaginary frequency appears [36]. It turns out that [O, O] and [O, NH] rings (compounds **1**, **2**, **3**, **5a**, **5b**, **5d**, **5d′**, **6b**, **8**, **9**, **12** and **18**) are systematically predicted to be planar while, on the other hand, sulfur containing dyes always have a non-planar ground-state geometry (**5c**, **5c′**, **6c**, **7c**, **10**, **13**, **14**, **15** and **19**). For instance, the deformations for the compounds **14**, **15** and **7c**, respectively, are 5.5°, 5.2° and 6.6° out of the plane antisymmetrical distortions. A constrained planar optimization actually leads to an energetic minimum, but the corresponding Hessian matrix shows negative eigen values, though the relative stability of distorted molecules with respect to planar structures is rather limited (it is less than 1 kcal mol^{-1} for **5a** and **7c**).

3.2. Absorption spectra and solvent effects

From our TD-DFT and PCM-TD-DFT results [37], we conclude that for the selected set of 1,2-cyclized and 1,2-3,4-dicyclized derivatives, the first excited state originates from a HOMO to LUMO transition that corresponds to the λ_{max} absorption band in the visible spectrum. In the gas phase, the inspection of these frontier levels, when going from the 1,2,3,4-tetrafluoro-AQ (**1**) to the entire set of substituted dyes, shows that the LUMO stays fairly stable, unlike the HOMO level (Table 3). The fluctuations of the HOMO when changing the side groups induce the variability of the transition energy and finally lead to a nice covering of a wide λ_{max} window, from 342 nm to 660 nm. In Table 2, we have indexed the calculated λ_{max} with the INDO [4], TD-B3LYP/PBE0 and CH_2Cl_2-TD-B3LYP/PBE0 methodologies. There is no surprise that our DFT approaches perform better than the early semi-empirical results [4]: our largest discrepancies are 102 nm for both B3LYP (molecule **5b**) and PBE0 (molecule **15**), while the largest discrepancy is evaluated to 254 nm for INDO (**8**). If we turn to the average differences

Table 2
Comparative λ_{max} (in nm) provided by INDO, TD-B3LYP, TD-PBE0 and MLR methods, in gaseous phase and including solvent effects (PCM)

	GAZ			CH_2Cl_2			
	λ_{max}^{INDO}	λ_{max}^{PBE0}	λ_{max}^{B3LYP}	λ_{max}^{PBE0}	λ_{max}^{B3LYP}	λ_{max}^{MLR}	$\lambda_{max}^{Exp.}$ (Ref. [4])
AQ (Ref. [38])	–	306	318	316	327	–	325
1	–	323	334	330	342	303	329
2	–	470	485	476	491	494	499
3	–	357	372	360	374	336	355
5a	453	523	546	554	579	564	550
5b	351	432	455	455	481	417	353
5c	458	549	574	576	604	599	579
5c′	456	566	593	587	617	601	588
5d	426	459	474	489	505	508	516
5e	418	481	498	511	529	530	535
6a	490	556	579	595	620	617	591
6b	423	483	502	503	526	497	490
6b′	419	471	487	476	491	494	497
6c	496	582	607	618	646	653	619
7c	470	566	594	590	621	601	582, *354*
8	388, 518	550	567	577	594	583	642, *592*
9	334, 460	525	546	553	576	567	567, *389*
10	388, 526	569	586	596	613	618	664, *611*
11	429, 554	534	552	560	578	594	620, *574*
12	370	446	467	468	491	448	414
13	330, 467	550	572	574	599	610	592, *414*
14	393, 543	592	610	621	639	653	689, *633*
15	402, 561	610	630	640	660	702	712, *656*
18	–	497	524	526	552	516	–
19	–	501	528	497	524	471	–
20	–	529	553	564	591	565	–
21	–	636	655	671	691	745	–
22	–	628	646	667	689	731	–
23	–	640	660	675	696	747	–
1,4-diNH_2-AQ	–	506	518	542	529	710	582
1,4,5,8-tetraNH_2-AQ	–	568	582	577	604	583	619

Experimentally, for some of the studied compounds, a second λ_{max} with a comparatively smaller oscillator strength is observed. (They are indicated in italic in the table.)

between theoretical λ_{max} vs experimental values, a good improvement with respect to semi-empirical results also shows up: from a 123-nm standard deviation for INDO/S, down to 48 nm and 36 nm for PBE0 and B3LYP, respectively. The latter systematically overestimates the λ_{max} while the former one slightly underestimates them.

The introduction of the solvent effects (PCM model) in our TD-DFT calculation leads to a large batho-shift for all λ_{max} values, that can be estimated to $\sim$70–80 nm. Including dichloromethane effects induces a decrease in the standard deviation to 31 nm and 34 nm for PBE0 and B3LYP, respectively, despite the fact that the largest discrepancy increases (128 nm for B3LYP and 102 nm for PBE0). Moreover, for the largest systems, the sensibility of λ_{max} to the solvent decreases. For instance, for compound **19**, one can see that there is no drastic displacement of the UV/VIS spectrum (+3 nm) when solvent effects are taken into account. An explanation is that the accessibility of the dye chromophoric and auxochromic units by the solvent molecules is lower for the sterically jammed compounds or when bulky ligands are aside the chromophoric unit. Thus, small dyes have their excited electronic structure (relatively) more stabilized by the solvent and the result is a larger batho-shift of their UV/VIS spectrum. In gaseous phase, the HOMO–LUMO energy gap gives a good idea of the shift: the larger the gap, the larger is the hypso-shift. Unfortunately, the same approximation doesn't hold when one takes into account the solvent effects. Nevertheless, as these effects have definitely to be taken into account, the following discussions will always be based on PCM-TD-DFT results.

By using MLR, one can find an equation that combines the values in such a way that the experimental values are optimally reproduced (Eq. (2)):

$$\lambda_{max}^{MLR} = -106.0 - 4.4\lambda_{max}^{B3LYP} + 5.8\lambda_{max}^{PBE0} \quad (2)$$

This equation provides an adjusted R^2 of 94.2% and each parameter is statistically significant within a 99% level of confidence, meaning that no parameter has to be removed. Fig. 2 shows that MLR performs better: the standard deviation is falling down to 25 nm. Moreover, it allows to limit the largest theory/experiment discrepancies to relatively small values (63 nm for **5b** and 60 nm for **8**). The efficiency of our model can be explained by the fact that: (i) the solvent effects are taken into account, (ii) the 6-31G(d,p) basis set already allows an early intramolecular interaction description, i.e., the hydrogen bonds between the carbonyl chromophoric unit and the amino (–NHR) groups (**5a**, **5c**, **6a**, **6c**, **7c**, **8**, **10**, **11**, **13**, **14** and **15**). These effects play an important role for the λ_{max} bathochromic

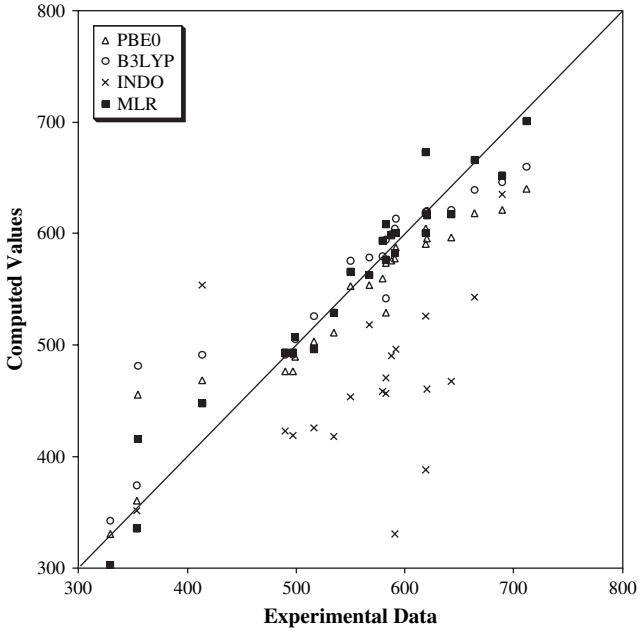

Fig. 2. Confrontation between the experiment with the λ_{max} (in nm) calculated with INDO method, the PCM(CH_2Cl_2)-TD-B3LYP, PCM(CH_2Cl_2)-TD-PBE0 methods and their MLR combinations.

shift [6] in anthraquinone derivatives. It is also important to underline that, as expected from energetical considerations, the distorted geometries have an absorption λ_{max} which is in better agreement with respect to the experimental figures than any constrained planar structures. Indeed, the latter systemically produce too high λ_{max} values. Including solvent effect, we have 576 nm for compound **5c**, in better agreement with the experiment (579 nm) than the **5c** planar (583 nm). The loss of planarity goes along with a loss of electronic delocalization which in turn hinders a large charge transfer during the electronic excitation.

3.3. Substitution effects

Actually, for the substituents that do not allow any hydrogen bond with C═O, the λ_{max} is a function of the electron availability: the stronger the donor character of the hetaryl moieties, the more electrons pushed into the AQ rings, the larger λ_{max}, qualitatively ranking: S (+277 nm) > N (+228 nm) > O (+28 nm) (**20**, **18**, **5b**). The electron-donating strength of the oxygen substitution cannot be achieved through the [O, O] ring derivatives, due to the poor accuracy on these systems (**12**, **5b**). It turns out that even if the presence of sulfur atoms in the cycle brings the loss of planarity of the dye, there is a large batho-shift for this substitution probably due to the very polarizable character of this atom.

For compounds showing hydrogen bonds with the chromophoric unit (**5a**, **5c**, **6a**, **6c**, **7c**, **8**, **10**, **11**, **13**, **14** and **15**), the carbonyl bond length $d_{C=O}$, as well as the partial average atomic charge borne by the oxygen atoms (q^O) are properties (Table 3) that advantageously refine the trends given by the HOMO–LUMO gap to predict the shift direction and its amplitude. The knowledge of these properties allows to smartly shortcut the physics underlying the electronic excitation process by chasing similarities between ground state and excited state characteristics. As expected, the λ_{max} is dependent on two major factors: (i) the increasing number of hydrogen bonds with the C═O provides larger batho-shift, and (ii) the "proton availability" of each substitution, i.e., the stronger the acidic character, the larger the λ_{max}: −OH (+137 nm) > −NH (+48 nm) (**6b**, **5a**). It turns out that even if the hydroxy is a poor electron-donating group, it is the best proton-donating group, bringing a large change in $d_{C=O}$ and q^O. Moreover, the shifts become smaller and insensitive to the nature of the group when substitutions occur in 1,2-3,4-dicyclized derivatives (there are no drastic changes in $d_{C=O}$ and q^O when one goes from compound **21** to **23**). As an example, adding a 1,4-NH_2 to AQ results in a +226 nm shift compared to a +54 nm shift in 1,2-3,4-dicyclized derivatives (**23**). This can be understood as the [NH, NH] substitution in tetrafluoro-AQ is strong and always constitutes the main effect. Consequently, the groups added in 5–8 positions in dicyclized derivatives can be used for a fine tuning of the visible spectra. Comparing the effect of the electron-donating character and hydrogen bonds on the electronic spectra, one has to conclude that: (i) the electron-donating character of the sulfur atom has a large effect on the spectra displacement, (ii) we get a much larger batho-shift with dyes including atoms which could provide a good electron delocalization and have at least one acidic hydrogen in position 1, 4, 5 or 8. This is checked with **6a**, **6c**, **11**, **14**, **15**, **21**, **22**, **23** and **25**, where one finds the sulfur or the amine in position 1, 4, 5 or 8, that builds hydrogen bonds with C^+-O^-. Indeed, in Table 3, one can see that these molecules correspond to the largest changes in $d_{C=O}$ and q^O. For these compounds, we see a ±4% increase in $d_{C=O}$ and ±50% increase in q^O.

4. Conclusions and outlook

We have computed with a PCM-TD-DFT approach, the λ_{max} of several substituted fluoro-anthraquinones. It turns out that: (i) solvent strongly affects the UV/VIS spectrum (bathochromic effects) and has to be taken into account in the model. (ii) Derivatives including sulfur atoms in their cycle present a non-planar ground-state geometry. However, although the sulfur leads to non-planar structures, these dyes show the largest batho-shift (compared to O and N) probably due to the very polarizable character of sulfur. (iii) As expected, the presence of hydrogen bonds implying the carbonyl chromophoric units yields the strongest modifications in the geometries and charges, and subsequently in the excitation spectra. (iv) Combining the B3LYP and PBE0 results using an MLR approach produces λ_{max} that are in better agreement with experiment than any of the two functionals taken separately and significantly reduces the largest discrepancies with respect to experimental values. The proposed equation should therefore predict the λ_{max} of yet-to-synthesize dyes in the same family with minimum of ~25 nm accuracy.

In order to completely define the colour of a dye, one needs the energy and the oscillator strength of the first dipole-allowed transition, but of course the evaluation of additional parameters

Table 3
Average C=O bond length (in Å), average Mulliken charge on the oxygen (in *e*), and HOMO–LUMO energy levels (in eV) calculated with PBE0 and PCM(CH_2Cl_2)-PBE0

	HOMO		LUMO		$d_{C=O}$	q^O	
	GAZ	CH_2Cl_2	GAZ	CH_2Cl_2	GAZ	GAZ	CH_2Cl_2
AQ	–	–	–	–	1.230	−0.480	−0.510
1	−7.24	−7.55	−3.10	−3.00	1.223	−0.458	−0.497
2	−6.46	−6.34	−3.35	−3.20	1.246	−0.557	−0.582
3	−7.48	−7.37	−3.30	−3.15	1.219	−0.436	−0.474
5a	−5.62	−5.56	−2.77	−2.81	1.235	−0.520	−0.540
5b	−6.23	−6.16	−2.76	−2.82	1.224	−0.465	−0.502
5c	−5.55	−5.51	−2.85	−2.87	1.236	−0.520	−0.550
5c′	−5.31	−5.34	−2.73	−2.79	1.237	−0.530	−0.560
5d	−5.63	−5.60	−2.43	−2.55	1.236	−0.520	−0.560
5e	−5.62	−5.60	−2.5	−2.62	1.235	−0.516	−0.530
6a	−5.71	−5.57	−3.04	−3.00	1.258	−0.620	−0.630
6b	−6.13	−6.08	−3.05	−3.03	1.248	−0.563	−0.585
6b′	−5.25	−5.52	−3.06	−3.06	1.247	−0.562	−0.587
6c	−5.63	−5.52	−3.10	−3.06	1.259	−0.616	−0.632
7c	−5.63	−3.04	−5.54	−3.01	1.230	−0.499	−0.529
8	−5.13	−5.19	−2.45	−2.60	1.251	−0.582	−0.606
9	−5.35	−5.40	−2.52	−2.64	1.237	−0.525	−0.554
10	−5.11	−5.18	−2.55	−2.66	1.252	−0.586	−0.608
11	−4.86	−5.01	−2.12	−2.31	1.251	−0.550	−0.612
12	−5.87	−5.93	−2.50	−2.66	1.226	−0.472	−0.506
13	−5.31	−5.36	−2.59	−2.71	1.238	−0.526	−0.553
14	−5.15	−5.20	−2.70	−2.80	1.252	−0.585	−0.605
15	−5.26	−5.29	−2.85	−2.90	1.247	−0.565	−0.585
18	−5.64	−5.53	−2.57	−2.64	1.226	−0.473	−0.513
19	−6.04	−6.18	−2.85	−2.48	1.228	−0.468	−0.497
20	−5.54	−5.58	−2.70	−2.98	1.226	−0.485	−0.522
21	−5.27	−5.27	−2.94	−2.98	1.264	−0.643	−0.650
22	−5.23	−5.25	−2.92	−2.95	1.275	−0.685	−0.691
23	−4.75	−4.77	−2.45	−2.56	1.267	−0.659	−0.667
1,4-diNH_2-AQ	−5.18	−5.22	−2.31	−2.44	1.247	−0.568	−0.597
1,4,5,8-tetraNH_2-AQ	−7.20	−4.62	−1.98	−2.12	1.265	−0.647	−0.660

like vibrational effects is necessary, especially for the 1,4-diNH-R substitution [6,10]. We are currently investigating this electron–phonon coupling by using tailored theoretical tools.

Acknowledgements

J. P. acknowledges the FRIA (Belgian "Fonds pour la formation à la Recherche dans L'Industrie et dans l'Agriculture") for his PhD grant. D. J. and E. A. P. thank the Belgian National Fund for their respective Research Associate positions. The authors thank Dr. Valérie Wathelet for her participation in statistical calculation. The calculations have been performed on the Interuniversity Scientific Computing Facility (ISCF), installed at the Facultés Universitaires Notre-Dame de la Paix (Namur, Belgium), for which the authors gratefully acknowledge the financial support of the FNRS-FRFC and the "Loterie Nationale" for the convention number 2.4578.02 and of the FUNDP.

References

[1] Green FJ. The Sigma-Aldrich handbook of stains, dyes and indicators. Milwaukee, WI: Aldrich Chemical Company, Inc.; 1990.
[2] Perkins AG, Everest AE. The natural organic coloring matters. London: Longmans; 1918.
[3] Christie RM. Colour chemistry. Cambridge: Royal Society of Chemistry; 2001.
[4] Matsui M, Tniguchi S, Suzuki M, Wang M, Funabiki K, Shiozaki H. Dyes Pigments 2005;65:211.
[5] Schäfer A. In: Grotendorst J, editor. Modern methods and algorithms of quantum chemistry. 2nd ed. NIC, vol. 3. Jülich: John von Neumann Institute for Computing; 2000.
[6] Jacquemin D, Preat J, Charlot M, Wathelet V, André JM, Perpete EA. J Chem Phys 2004;121:1736.
[7] Cossi M, Barone V. J Chem Phys 2001;115:4708.
[8] Adamo C, Barone V. Chem Phys Lett 2000;330:152.
[9] Baerends EJ, Ricciardi G, Rosa A, van Gisbergen SJA. Coord Chem Rev 2002;230:5.
[10] Jacquemin D, Preat J, Wathelet V, André JM, Perpète EA. Chem Phys Lett 2005;405:429.
[11] Jamorski-Jödicke C, Lüthi HP. J Am Chem Soc 2002;125:252.
[12] Wilberg KB, de Oliveria AE, Trucks G. J Phys Chem A 2002; 106:4192.
[13] Yamaguchi Y. J Chem Phys 2002;117:4157.
[14] Infante I, Lelj F. Chem Phys Lett 2003;367:308.
[15] Parac M, Grimme S. Chem Phys 2003;29:11.
[16] Jsaworska M, Kazibut G, Lodowski P. J Phys Chem A 2003;107:1339.
[17] Guillaumont D, Nakamura S. Dyes Pigments 2000;46:85.
[18] Frisch MJ, Trucks GW, Schlegel HB, Gill PMW, Johnson BG, Robb MA, et al. GAUSSIAN 03 Revision B. 04. Pittsburgh, PA: Gaussian Inc.; 2003.
[19] Becke AD. Phys Rev A 1988;38:3098.
[20] Lee C, Yang W, Parr RG. Phys Rev B 1988;37:785.
[21] Perdew J, Burke K, Ernzerhof M. Phys Rev Lett 1997;78:1396.
[22] Perdew J, Burke K, Ernzerhof M. Phys Rev Lett 1996;77:3865.

[23] Becke AD. J Chem Phys 1993;98:5648.
[24] Adamo C, Barone V. J Chem Phys 1999;110:6158; Adamo C, Scuseria GE, Barone V. J Chem Phys 1999;11:2889.
[25] Perdew JP, Chevary JA, Vosko SH, Jackson KA, Pederson MR, Singh DJ, et al. Phys Rev B 1992;46:6671; Perdew JP, Burke R, Wang Y. Phys Rev B 1996;54:16533.
[26] Hariharan PC, Pople JA. Theor Chim Acta 1973;28:213.
[27] Amovilli C, Barone V, Cammi R, Cancès E, Cossi M, Mennucci B, et al. Adv Quantum Chem 1998;32:227.
[28] Dagnelie P. Statistique Théorique et Appliquée. Tome 1. Statistique descriptive et Bases de l'Inférence Statistique. Bruxelles: De Boeck and Larcier; 1998.
[29] Dagnelie P. Statistique Théorique et Appliquée. Tome 2. Inférence Statistique une et deux dimensions. Bruxelles: De Boeck and Larcier; 1998.
[30] Pollard J. A handbook of numerical and statistical techniques. Cambridge, UK: Cambridge University Press; 1979.
[31] Statgraphics Plus 5.1. Manugistics Inc.; 2000.
[32] Giles CH, Shah CD. Trans Faraday Soc 1969;65:2508.
[33] Wegerle D. J Soc Dyers Colour 1973;89:54.
[34] Sinclair RS, Mc Alpine E. J Soc Dyers Colour 1975;91:399.
[35] Itskovich EM, Krutovskaya IV, Rodonova GN, Sheban GV. Opt Spektrosk 1983;55:454.
[36] For the larger molecules 14–19, the frequencies calculations have not been done because too much CPU resources are needed. However, its of interest to see the non-planarity is due to the presence of at least one sulfur in the aromatic cycle of the dyes **14**–**17**. It is thus reasonable to think that these compounds should have a non-planar ground state geometry.
[37] For technical reasons, it was impossible to calculate the excitation energies for the compound **17** [4] because of a numerical instability during the RPA calculation.
[38] UV-spectra taken in dichloromethane with *PERKIN ELMER Lambda 6 Scanning UV spectrometer*.